

**Azimuthal anisotropy of  $\pi^0$  production in Au+Au collisions at  $\sqrt{s_{NN}} = 200$  GeV:  
Path-length dependence of jet-quenching and the role of initial geometry**

A. Adare,<sup>11</sup> S. Afanasiev,<sup>26</sup> C. Aidala,<sup>39</sup> N.N. Ajitanand,<sup>56</sup> Y. Akiba,<sup>50,51</sup> H. Al-Bataineh,<sup>45</sup> J. Alexander,<sup>56</sup> K. Aoki,<sup>32,50</sup> Y. Aramaki,<sup>10</sup> E.T. Atomssa,<sup>33</sup> R. Averbeck,<sup>57</sup> T.C. Awes,<sup>46</sup> B. Azmoun,<sup>5</sup> V. Babintsev,<sup>22</sup> M. Bai,<sup>4</sup> G. Baksay,<sup>18</sup> L. Baksay,<sup>18</sup> K.N. Barish,<sup>6</sup> B. Bassalleck,<sup>44</sup> A.T. Basye,<sup>1</sup> S. Bathe,<sup>6</sup> V. Baublis,<sup>49</sup> C. Baumann,<sup>40</sup> A. Bazilevsky,<sup>5</sup> S. Belikov,<sup>5,\*</sup> R. Belmont,<sup>61</sup> R. Bennett,<sup>57</sup> A. Berdnikov,<sup>53</sup> Y. Berdnikov,<sup>53</sup> A.A. Bickley,<sup>11</sup> J.S. Bok,<sup>64</sup> K. Boyle,<sup>57</sup> M.L. Brooks,<sup>35</sup> H. Buesching,<sup>5</sup> V. Bumazhnov,<sup>22</sup> G. Bunce,<sup>5,51</sup> S. Butsyk,<sup>35</sup> C.M. Camacho,<sup>35</sup> S. Campbell,<sup>57</sup> C.-H. Chen,<sup>57</sup> C.Y. Chi,<sup>12</sup> M. Chiu,<sup>5</sup> I.J. Choi,<sup>64</sup> R.K. Choudhury,<sup>3</sup> P. Christiansen,<sup>37</sup> T. Chujo,<sup>60</sup> P. Chung,<sup>56</sup> O. Chvala,<sup>6</sup> V. Cianciolo,<sup>46</sup> Z. Citron,<sup>57</sup> B.A. Cole,<sup>12</sup> M. Connors,<sup>57</sup> P. Constantin,<sup>35</sup> M. Csanád,<sup>16</sup> T. Csörgő,<sup>29</sup> T. Dahms,<sup>57</sup> S. Dairaku,<sup>32,50</sup> I. Danchev,<sup>61</sup> K. Das,<sup>19</sup> A. Datta,<sup>39</sup> G. David,<sup>5</sup> A. Denisov,<sup>22</sup> A. Deshpande,<sup>51,57</sup> E.J. Desmond,<sup>5</sup> O. Dietzsch,<sup>54</sup> A. Dion,<sup>57</sup> M. Donadelli,<sup>54</sup> O. Drapier,<sup>33</sup> A. Drees,<sup>57</sup> K.A. Drees,<sup>4</sup> J.M. Durham,<sup>57</sup> A. Durum,<sup>22</sup> D. Dutta,<sup>3</sup> S. Edwards,<sup>19</sup> Y.V. Efremenko,<sup>46</sup> F. Ellinghaus,<sup>11</sup> T. Engelmöre,<sup>12</sup> A. Enokizono,<sup>34</sup> H. En'yo,<sup>50,51</sup> S. Esumi,<sup>60</sup> B. Fadem,<sup>41</sup> D.E. Fields,<sup>44</sup> M. Finger, Jr.,<sup>7</sup> M. Finger,<sup>7</sup> F. Fleuret,<sup>33</sup> S.L. Fokin,<sup>31</sup> Z. Fraenkel,<sup>63,\*</sup> J.E. Frantz,<sup>57</sup> A. Franz,<sup>5</sup> A.D. Frawley,<sup>19</sup> K. Fujiwara,<sup>50</sup> Y. Fukao,<sup>50</sup> T. Fusayasu,<sup>43</sup> I. Garishvili,<sup>58</sup> A. Glenn,<sup>11</sup> H. Gong,<sup>57</sup> M. Gonin,<sup>33</sup> Y. Goto,<sup>50,51</sup> R. Granier de Cassagnac,<sup>33</sup> N. Grau,<sup>12</sup> S.V. Greene,<sup>61</sup> M. Grosse Perdekamp,<sup>23,51</sup> T. Gunji,<sup>10</sup> H.-Å. Gustafsson,<sup>37,\*</sup> J.S. Haggerty,<sup>5</sup> K.I. Hahn,<sup>17</sup> H. Hamagaki,<sup>10</sup> J. Hamblen,<sup>58</sup> J. Hanks,<sup>12</sup> R. Han,<sup>48</sup> E.P. Hartouni,<sup>34</sup> E. Haslum,<sup>37</sup> R. Hayano,<sup>10</sup> M. Heffner,<sup>34</sup> S. Hegyi,<sup>29</sup> T.K. Hemmick,<sup>57</sup> T. Hester,<sup>6</sup> X. He,<sup>20</sup> J.C. Hill,<sup>25</sup> M. Hohlmann,<sup>18</sup> W. Holzmann,<sup>12</sup> K. Homma,<sup>21</sup> B. Hong,<sup>30</sup> T. Horaguchi,<sup>21</sup> D. Hornback,<sup>58</sup> S. Huang,<sup>61</sup> T. Ichihara,<sup>50,51</sup> R. Ichimiya,<sup>50</sup> J. Ide,<sup>41</sup> Y. Ikeda,<sup>60</sup> K. Imai,<sup>32,50</sup> M. Inaba,<sup>60</sup> D. Isenhower,<sup>1</sup> M. Ishihara,<sup>50</sup> T. Isobe,<sup>10</sup> M. Issah,<sup>61</sup> A. Isupov,<sup>26</sup> D. Ivanischev,<sup>49</sup> B.V. Jacak,<sup>57,†</sup> J. Jia,<sup>5,56</sup> J. Jin,<sup>12</sup> B.M. Johnson,<sup>5</sup> K.S. Joo,<sup>42</sup> D. Jouan,<sup>47</sup> D.S. Jumper,<sup>1</sup> F. Kajihara,<sup>10</sup> S. Kametani,<sup>50</sup> N. Kamihara,<sup>51</sup> J. Kamin,<sup>57</sup> J.H. Kang,<sup>64</sup> J. Kapustinsky,<sup>35</sup> D. Kawall,<sup>39,51</sup> M. Kawashima,<sup>52,50</sup> A.V. Kazantsev,<sup>31</sup> T. Kempel,<sup>25</sup> A. Khanzadeev,<sup>49</sup> K.M. Kijima,<sup>21</sup> B.I. Kim,<sup>30</sup> D.H. Kim,<sup>42</sup> D.J. Kim,<sup>27</sup> E.J. Kim,<sup>8</sup> E. Kim,<sup>55</sup> S.H. Kim,<sup>64</sup> Y.J. Kim,<sup>23</sup> E. Kinney,<sup>11</sup> K. Kiriluk,<sup>11</sup> Á. Kiss,<sup>16</sup> E. Kistenev,<sup>5</sup> L. Kochenda,<sup>49</sup> B. Komkov,<sup>49</sup> M. Konno,<sup>60</sup> J. Koster,<sup>23</sup> D. Kotchetkov,<sup>44</sup> A. Kozlov,<sup>63</sup> A. Král,<sup>13</sup> A. Kravitz,<sup>12</sup> G.J. Kunde,<sup>35</sup> K. Kurita,<sup>52,50</sup> M. Kurosawa,<sup>50</sup> Y. Kwon,<sup>64</sup> G.S. Kyle,<sup>45</sup> R. Lacey,<sup>56</sup> Y.S. Lai,<sup>12</sup> J.G. Lajoie,<sup>25</sup> A. Lebedev,<sup>25</sup> D.M. Lee,<sup>35</sup> J. Lee,<sup>17</sup> K.B. Lee,<sup>30</sup> K. Lee,<sup>55</sup> K.S. Lee,<sup>30</sup> M.J. Leitch,<sup>35</sup> M.A.L. Leite,<sup>54</sup> E. Leitner,<sup>61</sup> B. Lenzi,<sup>54</sup> P. Liebing,<sup>51</sup> L.A. Linden Levy,<sup>11</sup> T. Liška,<sup>13</sup> A. Litvinenko,<sup>26</sup> H. Liu,<sup>35,45</sup> M.X. Liu,<sup>35</sup> X. Li,<sup>9</sup> B. Love,<sup>61</sup> R. Luechtenborg,<sup>40</sup> D. Lynch,<sup>5</sup> C.F. Maguire,<sup>61</sup> Y.I. Makdisi,<sup>4</sup> A. Malakhov,<sup>26</sup> M.D. Malik,<sup>44</sup> V.I. Manko,<sup>31</sup> E. Mannel,<sup>12</sup> Y. Mao,<sup>48,50</sup> H. Masui,<sup>60</sup> F. Matathias,<sup>12</sup> M. McCumber,<sup>57</sup> P.L. McGaughey,<sup>35</sup> N. Means,<sup>57</sup> B. Meredith,<sup>23</sup> Y. Miake,<sup>60</sup> A.C. Mignerey,<sup>38</sup> P. Mikeš,<sup>7,24</sup> K. Miki,<sup>60</sup> A. Milov,<sup>5</sup> M. Mishra,<sup>2</sup> J.T. Mitchell,<sup>5</sup> A.K. Mohanty,<sup>3</sup> Y. Morino,<sup>10</sup> A. Morreale,<sup>6</sup> D.P. Morrison,<sup>5</sup> T.V. Moukhanova,<sup>31</sup> J. Murata,<sup>52,50</sup> S. Nagamiya,<sup>28</sup> J.L. Nagle,<sup>11</sup> M. Naglis,<sup>63</sup> M.I. Nagy,<sup>16</sup> I. Nakagawa,<sup>50,51</sup> Y. Nakamiya,<sup>21</sup> T. Nakamura,<sup>21,28</sup> K. Nakano,<sup>50,59</sup> J. Newby,<sup>34</sup> M. Nguyen,<sup>57</sup> R. Nouicer,<sup>5</sup> A.S. Nyanin,<sup>31</sup> E. O'Brien,<sup>5</sup> S.X. Oda,<sup>10</sup> C.A. Ogilvie,<sup>25</sup> K. Okada,<sup>51</sup> M. Oka,<sup>60</sup> Y. Onuki,<sup>50</sup> A. Oskarsson,<sup>37</sup> M. Ouchida,<sup>21</sup> K. Ozawa,<sup>10</sup> R. Pak,<sup>5</sup> V. Pantuev,<sup>57</sup> V. Papavassiliou,<sup>45</sup> I.H. Park,<sup>17</sup> J. Park,<sup>55</sup> S.K. Park,<sup>30</sup> W.J. Park,<sup>30</sup> S.F. Pate,<sup>45</sup> H. Pei,<sup>25</sup> J.-C. Peng,<sup>23</sup> H. Pereira,<sup>14</sup> V. Peresedov,<sup>26</sup> D.Yu. Peressounko,<sup>31</sup> C. Pinkenburg,<sup>5</sup> R.P. Pisani,<sup>5</sup> M. Proissl,<sup>57</sup> M.L. Purschke,<sup>5</sup> A.K. Purwar,<sup>35</sup> H. Qu,<sup>20</sup> J. Rak,<sup>27</sup> A. Rakotozafindrabe,<sup>33</sup> I. Ravinovich,<sup>63</sup> K.F. Read,<sup>46,58</sup> K. Reygers,<sup>40</sup> V. Riabov,<sup>49</sup> Y. Riabov,<sup>49</sup> E. Richardson,<sup>38</sup> D. Roach,<sup>61</sup> G. Roche,<sup>36</sup> S.D. Rolnick,<sup>6</sup> M. Rosati,<sup>25</sup> C.A. Rosen,<sup>11</sup> S.S.E. Rosendahl,<sup>37</sup> P. Rosnet,<sup>36</sup> P. Rukoyatkin,<sup>26</sup> P. Ružička,<sup>24</sup> B. Sahlmueller,<sup>40</sup> N. Saito,<sup>28</sup> T. Sakaguchi,<sup>5</sup> K. Sakashita,<sup>50,59</sup> V. Samsonov,<sup>49</sup> S. Sano,<sup>10,62</sup> T. Sato,<sup>60</sup> S. Sawada,<sup>28</sup> K. Sedgwick,<sup>6</sup> J. Seele,<sup>11</sup> R. Seidl,<sup>23</sup> A.Yu. Semenov,<sup>25</sup> R. Seto,<sup>6</sup> D. Sharma,<sup>63</sup> I. Shein,<sup>22</sup> T.-A. Shibata,<sup>50,59</sup> K. Shigaki,<sup>21</sup> M. Shimomura,<sup>60</sup> K. Shoji,<sup>32,50</sup> P. Shukla,<sup>3</sup> A. Sickles,<sup>5</sup> C.L. Silva,<sup>54</sup> D. Silvermyr,<sup>46</sup> C. Silvestre,<sup>14</sup> K.S. Sim,<sup>30</sup> B.K. Singh,<sup>2</sup> C.P. Singh,<sup>2</sup> V. Singh,<sup>2</sup> M. Slunečka,<sup>7</sup> R.A. Soltz,<sup>34</sup> W.E. Sondheim,<sup>35</sup> S.P. Sorensen,<sup>58</sup> I.V. Sourikova,<sup>5</sup> N.A. Sparks,<sup>1</sup> P.W. Stankus,<sup>46</sup> E. Stenlund,<sup>37</sup> S.P. Stoll,<sup>5</sup> T. Sugitate,<sup>21</sup> A. Sukhanov,<sup>5</sup> J. Sziklai,<sup>29</sup> E.M. Takagui,<sup>54</sup> A. Taketani,<sup>50,51</sup> R. Tanabe,<sup>60</sup> Y. Tanaka,<sup>43</sup> K. Tanida,<sup>32,50,51</sup> M.J. Tannenbaum,<sup>5</sup> S. Tarafdar,<sup>2</sup> A. Taranenko,<sup>56</sup> P. Tarján,<sup>15</sup> H. Themann,<sup>57</sup> T.L. Thomas,<sup>44</sup> M. Togawa,<sup>32,50</sup> A. Toia,<sup>57</sup> L. Tomášek,<sup>24</sup> H. Torii,<sup>21</sup> R.S. Towell,<sup>1</sup> I. Tserruya,<sup>63</sup> Y. Tsuchimoto,<sup>21</sup> C. Vale,<sup>5,25</sup> H. Valle,<sup>61</sup> H.W. van Hecke,<sup>35</sup> E. Vazquez-Zambrano,<sup>12</sup> A. Veicht,<sup>23</sup> J. Velkovska,<sup>61</sup> R. Vértesi,<sup>15,29</sup> A.A. Vinogradov,<sup>31</sup> M. Virius,<sup>13</sup> V. Vrba,<sup>24</sup> E. Vznuzdaev,<sup>49</sup> X.R. Wang,<sup>45</sup> D. Watanabe,<sup>21</sup> K. Watanabe,<sup>60</sup> Y. Watanabe,<sup>50,51</sup> F. Wei,<sup>25</sup>

R. Wei,<sup>56</sup> J. Wessels,<sup>40</sup> S.N. White,<sup>5</sup> D. Winter,<sup>12</sup> J.P. Wood,<sup>1</sup> C.L. Woody,<sup>5</sup> R.M. Wright,<sup>1</sup> M. Wysocki,<sup>11</sup>  
 W. Xie,<sup>51</sup> Y.L. Yamaguchi,<sup>10</sup> K. Yamaura,<sup>21</sup> R. Yang,<sup>23</sup> A. Yanovich,<sup>22</sup> J. Ying,<sup>20</sup> S. Yokkaichi,<sup>50,51</sup>  
 G.R. Young,<sup>46</sup> I. Younus,<sup>44</sup> Z. You,<sup>48</sup> I.E. Yushmanov,<sup>31</sup> W.A. Zajc,<sup>12</sup> C. Zhang,<sup>46</sup> S. Zhou,<sup>9</sup> and L. Zolin<sup>26</sup>

(PHENIX Collaboration)

- <sup>1</sup>Abilene Christian University, Abilene, Texas 79699, USA  
<sup>2</sup>Department of Physics, Banaras Hindu University, Varanasi 221005, India  
<sup>3</sup>Bhabha Atomic Research Centre, Bombay 400 085, India  
<sup>4</sup>Collider-Accelerator Department, Brookhaven National Laboratory, Upton, New York 11973-5000, USA  
<sup>5</sup>Physics Department, Brookhaven National Laboratory, Upton, New York 11973-5000, USA  
<sup>6</sup>University of California - Riverside, Riverside, California 92521, USA  
<sup>7</sup>Charles University, Ovocný trh 5, Praha 1, 116 36, Prague, Czech Republic  
<sup>8</sup>Chonbuk National University, Jeonju 561-756, Korea  
<sup>9</sup>China Institute of Atomic Energy (CIAE), Beijing, People's Republic of China  
<sup>10</sup>Center for Nuclear Study, Graduate School of Science, University of Tokyo, 7-3-1 Hongo, Bunkyo, Tokyo 113-0033, Japan  
<sup>11</sup>University of Colorado, Boulder, Colorado 80309, USA  
<sup>12</sup>Columbia University, New York, New York 10027 and Nevis Laboratories, Irvington, New York 10533, USA  
<sup>13</sup>Czech Technical University, Zikova 4, 166 36 Prague 6, Czech Republic  
<sup>14</sup>Dapnia, CEA Saclay, F-91191, Gif-sur-Yvette, France  
<sup>15</sup>Debrecen University, H-4010 Debrecen, Egyetem tér 1, Hungary  
<sup>16</sup>ELTE, Eötvös Loránd University, H - 1117 Budapest, Pázmány P. s. 1/A, Hungary  
<sup>17</sup>Ewha Womans University, Seoul 120-750, Korea  
<sup>18</sup>Florida Institute of Technology, Melbourne, Florida 32901, USA  
<sup>19</sup>Florida State University, Tallahassee, Florida 32306, USA  
<sup>20</sup>Georgia State University, Atlanta, Georgia 30303, USA  
<sup>21</sup>Hiroshima University, Kagamiyama, Higashi-Hiroshima 739-8526, Japan  
<sup>22</sup>IHEP Protvino, State Research Center of Russian Federation, Institute for High Energy Physics, Protvino, 142281, Russia  
<sup>23</sup>University of Illinois at Urbana-Champaign, Urbana, Illinois 61801, USA  
<sup>24</sup>Institute of Physics, Academy of Sciences of the Czech Republic, Na Slovance 2, 182 21 Prague 8, Czech Republic  
<sup>25</sup>Iowa State University, Ames, Iowa 50011, USA  
<sup>26</sup>Joint Institute for Nuclear Research, 141980 Dubna, Moscow Region, Russia  
<sup>27</sup>Helsinki Institute of Physics and University of Jyväskylä, P.O.Box 35, FI-40014 Jyväskylä, Finland  
<sup>28</sup>KEK, High Energy Accelerator Research Organization, Tsukuba, Ibaraki 305-0801, Japan  
<sup>29</sup>KFKI Research Institute for Particle and Nuclear Physics of the Hungarian Academy of Sciences (MTA KFKI RMKI), H-1525 Budapest 114, POBox 49, Budapest, Hungary  
<sup>30</sup>Korea University, Seoul 136-701, Korea  
<sup>31</sup>Russian Research Center "Kurchatov Institute", Moscow, Russia  
<sup>32</sup>Kyoto University, Kyoto 606-8502, Japan  
<sup>33</sup>Laboratoire Leprince-Ringuet, Ecole Polytechnique, CNRS-IN2P3, Route de Saclay, F-91128, Palaiseau, France  
<sup>34</sup>Lawrence Livermore National Laboratory, Livermore, California 94550, USA  
<sup>35</sup>Los Alamos National Laboratory, Los Alamos, New Mexico 87545, USA  
<sup>36</sup>LPC, Université Blaise Pascal, CNRS-IN2P3, Clermont-Fd, 63177 Aubiere Cedex, France  
<sup>37</sup>Department of Physics, Lund University, Box 118, SE-221 00 Lund, Sweden  
<sup>38</sup>University of Maryland, College Park, Maryland 20742, USA  
<sup>39</sup>Department of Physics, University of Massachusetts, Amherst, Massachusetts 01003-9337, USA  
<sup>40</sup>Institut für Kernphysik, University of Muenster, D-48149 Muenster, Germany  
<sup>41</sup>Muhlenberg College, Allentown, Pennsylvania 18104-5586, USA  
<sup>42</sup>Myongji University, Yongin, Kyonggido 449-728, Korea  
<sup>43</sup>Nagasaki Institute of Applied Science, Nagasaki-shi, Nagasaki 851-0193, Japan  
<sup>44</sup>University of New Mexico, Albuquerque, New Mexico 87131, USA  
<sup>45</sup>New Mexico State University, Las Cruces, New Mexico 88003, USA  
<sup>46</sup>Oak Ridge National Laboratory, Oak Ridge, Tennessee 37831, USA  
<sup>47</sup>IPN-Orsay, Université Paris Sud, CNRS-IN2P3, BP1, F-91406, Orsay, France  
<sup>48</sup>Peking University, Beijing, People's Republic of China  
<sup>49</sup>PNPI, Petersburg Nuclear Physics Institute, Gatchina, Leningrad region, 188300, Russia  
<sup>50</sup>RIKEN Nishina Center for Accelerator-Based Science, Wako, Saitama 351-0198, JAPAN  
<sup>51</sup>RIKEN BNL Research Center, Brookhaven National Laboratory, Upton, New York 11973-5000, USA  
<sup>52</sup>Physics Department, Rikkyo University, 3-34-1 Nishi-Ikebukuro, Toshima, Tokyo 171-8501, Japan  
<sup>53</sup>Saint Petersburg State Polytechnic University, St. Petersburg, Russia  
<sup>54</sup>Universidade de São Paulo, Instituto de Física, Caixa Postal 66318, São Paulo CEP05315-970, Brazil  
<sup>55</sup>Seoul National University, Seoul 151-742, Korea  
<sup>56</sup>Chemistry Department, Stony Brook University, Stony Brook, SUNY, New York 11794-3400, USA  
<sup>57</sup>Department of Physics and Astronomy, Stony Brook University, SUNY, Stony Brook, New York 11794, USA

<sup>58</sup>University of Tennessee, Knoxville, Tennessee 37996, USA

<sup>59</sup>Department of Physics, Tokyo Institute of Technology, Oh-okayama, Meguro, Tokyo 152-8551, Japan

<sup>60</sup>Institute of Physics, University of Tsukuba, Tsukuba, Ibaraki 305, Japan

<sup>61</sup>Vanderbilt University, Nashville, Tennessee 37235, USA

<sup>62</sup>Waseda University, Advanced Research Institute for Science and Engineering, 17 Kikui-cho, Shinjuku-ku, Tokyo 162-0044, Japan

<sup>63</sup>Weizmann Institute, Rehovot 76100, Israel

<sup>64</sup>Yonsei University, IPAP, Seoul 120-749, Korea

(Dated: October 22, 2018)

We have measured the azimuthal anisotropy of  $\pi^0$  production for  $1 < p_T < 18$  GeV/c for Au+Au collisions at  $\sqrt{s_{\text{NN}}} = 200$  GeV. The observed anisotropy shows a gradual decrease for  $3 \lesssim p_T \lesssim 7-10$  GeV/c, but remains positive beyond 10 GeV/c. The magnitude of this anisotropy is under-predicted, up to at least  $\sim 10$  GeV/c, by current perturbative QCD (pQCD) energy-loss model calculations. An estimate of the increase in anisotropy expected from initial-geometry modification due to gluon saturation effects and fluctuations is insufficient to account for this discrepancy. Calculations that implement a path length dependence steeper than what is implied by current pQCD energy-loss models show reasonable agreement with the data.

PACS numbers: 25.75.Dw

A central goal of high-energy nuclear physics is to understand the properties of the strongly-coupled Quark Gluon Plasma (sQGP), a new form of nuclear matter identified at the Relativistic Heavy Ion Collider (RHIC) [1]. An important tool for this goal is jet quenching or the suppression of high transverse momentum ( $p_T$ ) hadron yields as a result of in-medium energy loss of high  $p_T$  jets [2]. Such suppression was first observed in measurements of the nuclear modification factor for single hadron yields  $R_{\text{AA}} = \frac{dN_{\text{AA}}}{\langle T_{\text{AA}} \rangle d\sigma_{\text{pp}}}$ , where  $dN_{\text{AA}}$  is the differential yield in Au+Au collisions,  $d\sigma_{\text{pp}}$  is the differential cross section in p+p collisions for given  $p_T$ , and  $\langle T_{\text{AA}} \rangle$  is the nuclear overlap integral for given Au+Au centrality bin [3]. Later on this effect was also observed in measurements of dihadron [4] and  $\gamma$ -hadron correlations [5].

Current theoretical descriptions of jet quenching are commonly based on a perturbative QCD (pQCD) framework [6], which assumes that the coupling of jets with the medium is weak, even though the medium itself is strongly-coupled. Prompted by the large amount of experimental data from RHIC, several sophisticated pQCD-based models have been developed in the last decade [2, 6]. These models have provided initial estimates of the properties of the sQGP, such as the momentum broadening per mean free path,  $\hat{q} = \langle k_T^2 \rangle / \lambda$ , and the energy loss per unit length,  $dE/dl$  [6–8].

Despite these successes, the pQCD description of jet quenching faces several challenges (see Ref [9]). Besides a large discrepancy among models of extracted medium properties such as  $\hat{q}$  [8], the energy-loss models also disagree in their predictions of the azimuthal anisotropy of high  $p_T$  hadrons [8]. The latter characterizes hadron emission relative to the reaction plane angle ( $\Psi_{\text{RP}}$ ),  $dN/d(\phi - \Psi_{\text{RP}}) \propto (1 + 2v_2 \cos(2(\phi - \Psi_{\text{RP}})))$ . Such azimuthal anisotropy ensues because the hadron yield is more suppressed along the long axis of the almond-shaped fireball than the short axis. Thus the magnitude

of the anisotropy,  $v_2$ , is sensitive to the path length ( $l$ ) dependence of energy loss, which scales as  $\Delta E \sim l$  for collisional energy loss [10],  $\Delta E \sim l^2$  for coherent radiative energy loss [10], and  $\Delta E \sim l^3$  for a non-perturbative energy loss calculation using AdS/CFT gravity-gauge dual theory [11]. However, our ability to probe such  $l$  dependences hinges not only on precision data at high  $p_T$ , but also on a good understanding of the role of the initial collision geometry. One geometry commonly used in energy-loss models is based on the Optical Glauber model [12], which assumes a smooth Woods-Saxon nuclear geometry. Such geometry ignores the event-by-event shape distortion due to spacial fluctuations of participating nucleons [13], and a possible overall shape distortion due to gluon saturation effects, *i.e.* the so called CGC geometry [14]. These effects have been shown to be important (up to 15-30% each) for elliptic flow at low  $p_T$  [15, 16]. However, their influences on jet quenching  $v_2$  at high  $p_T$  are not well studied to date.

In this Letter we present a new measurement of the  $\pi^0$  anisotropy in  $\sqrt{s_{\text{NN}}} = 200$  GeV Au+Au collisions. This measurement complements our prior results [17–19], but significantly increases both the  $p_T$  reach and the statistical precision above 6 GeV/c, allowing for quantitative comparisons to energy-loss models, as well as detailed investigations of the role of the initial collision geometry.

Results were obtained from  $\sim 3.5 \times 10^9$  minimum bias events taken in 2007. Event centrality was determined by the number of charged particles detected in the Beam-Beam Counters (BBC,  $3.0 < |\eta| < 3.9$ ). A Monte-Carlo (MC) Glauber model [12] was used to estimate the average number of participating nucleons ( $N_{\text{part}}$ ) and  $\langle T_{\text{AA}} \rangle$  for each centrality class.

Previous PHENIX analyses [19] estimated the RP using the charged particles detected in the BBC. Several new detectors, installed symmetrically on both sides of the beam line, provided additional RP measurements in

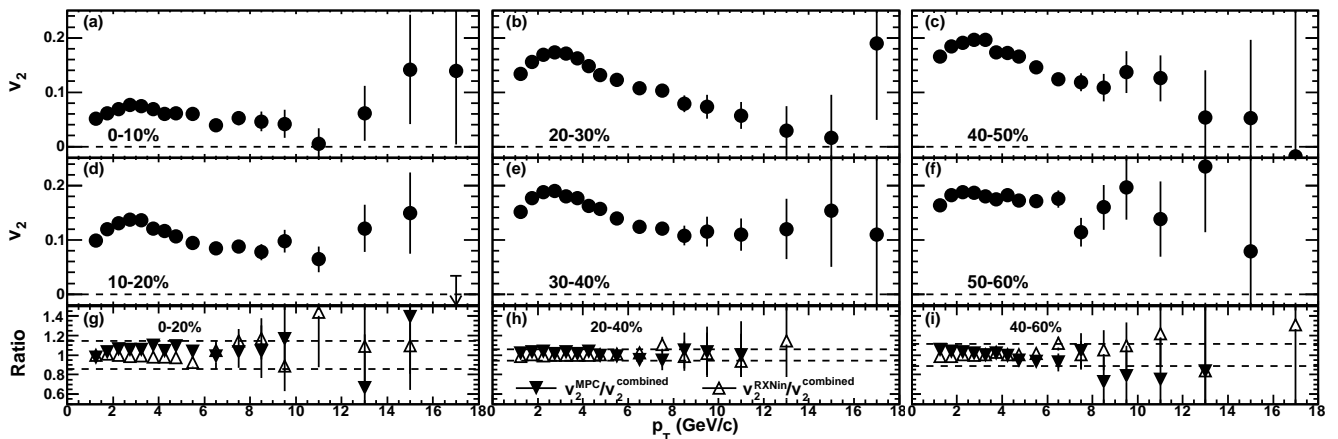


FIG. 1: (a)-(f):  $\pi^0$   $v_2$  using reaction plane determined with MPC and  $\text{RXN}_{\text{in}}$  combined as a function of  $p_T$  for different centralities. (g)-(i): ratios of  $v_2$  measured separately using MPC (solid triangles) and  $\text{RXN}_{\text{in}}$  (open triangles) to combined result; the dashed lines indicate the systematic error.

2007: the Muon Piston Calorimeters (MPC,  $3.1 < |\eta| < 3.9$ ) and the Reaction Plane detectors in two  $\eta$  ranges,  $\text{RXN}_{\text{in}}$  ( $\text{RXN}_{\text{out}}$ ) in  $1.5(1.0) < |\eta| < 2.8(1.5)$ . Each MPC is equipped with  $\text{PbWO}_4$  crystal scintillators to detect both charged and neutral particles. Each RXN consists of 12 azimuthally segmented paddle scintillators. This analysis estimates the RP angle using both the MPC and  $\text{RXN}_{\text{in}}$  to provide good resolution, while minimizing the potential biases from jets and dijets [20]. The error on the RP angle  $\Delta\Psi$ , and the RP dispersion factor  $\sigma_{\text{RP}} = \langle \cos 2\Delta\Psi \rangle$  are estimated by the sub-event method [19], giving  $\sigma_{\text{RP}} \sim 0.52$  and  $0.73$  in the central and mid-central collisions, respectively, which is  $\sim 80\%$  better than that for the BBCs. The large dataset and improved  $\sigma_{\text{RP}}$  give an equivalent of  $\sim 15$  fold increase in statistics over the previous measurement of  $v_2$  [19].

The methodology for  $v_2$  extraction follows our previous work [19]. We reconstruct the neutral pions via the  $\pi^0 \rightarrow \gamma + \gamma$  decay channel with photons detected in the Electromagnetic Calorimeter (EMC,  $|\eta| < 0.35$ ). We apply shower shape and pair asymmetry cuts to reduce the combinatorial background. The remaining background is subtracted by the mixed event method [19]. The azimuthal distribution of the  $\pi^0$  yields relative to the estimated RP angle,  $\Delta\phi = \phi - \Psi_{\text{RP}}$ , is divided into 6 bins in the interval of  $[0, \pi/2]$ , and fit to  $N_0(1 + 2v_2^{\text{raw}} \cos(2\Delta\phi))$ . The  $v_2$  is then obtained by applying the dispersion correction  $v_2 = v_2^{\text{raw}}/\sigma_{\text{RP}}$  for each centrality and  $p_T$  selection. The main sources of systematic uncertainties come from  $\sigma_{\text{RP}}$  and  $v_2^{\text{raw}}$ . The former is estimated by comparing measurements from different RP detectors, giving  $\sim 10\%$  for central and peripheral collisions and  $\sim 5\%$  for mid-central collisions. The latter accounts for the dependence of  $v_2$  on  $\pi^0$  identification cuts, as well as the variation among different sectors of EMC and different run groups, and is correlated in  $p_T$ ; it is estimated to be  $10\%$  for central collisions and  $3\%$  for other collisions.

Figure 1 (a)-(f) shows  $v_2(p_T)$  for six centrality bins, spanning 1-18 GeV/c. In the 10-50% centrality range, where the signal is large and the uncertainty is small, the  $v_2$  values above 3 GeV/c indicate a slow decrease up to 7-10 GeV/c, and remain significantly above zero at higher  $p_T$ . The ratios in Fig. 1 (g)-(i) confirm the consistency of  $v_2$  measured using the RP from the MPC or the  $\text{RXN}_{\text{in}}$  and imply that the influence of rapidity dependent jet bias to the RP, if any, is within the statistical or systematic uncertainty of the measurement.

Figure 2 (a)-(b) shows the centrality dependence of  $v_2$  in two high  $p_T$  selections. They are compared with four pQCD jet quenching model calculations, AMY, HT and ASW from [8] and WHDG from [22]. The WHDG model was calculated for gluon density  $dN/dg = 1000 - 1600$ , a range constrained by 0-5% ( $N_{\text{part}} = 351$ )  $\pi^0$   $R_{\text{AA}}$  data [7]. The calculation assumes analytical Woods-Saxon nuclear geometry with a longitudinal Bjorken expansion. The AMY, HT and ASW models were fitted independently to the 0-5%  $\pi^0$   $R_{\text{AA}}$  data [8]; they were implemented in a 3D ideal hydrodynamic code with identical initial Wood-Saxon nuclear geometry, medium evolution and fragmentation functions. The HT and ASW models include only coherent radiative energy loss, while the AMY and WHDG also include collisional energy loss. The ASW and WHDG models predict quite sizable, and similar  $v_2$ , while the HT and AMY models tend to give much smaller  $v_2$ . However, all models significantly underpredict the  $v_2$  data in  $6 < p_T < 9$  GeV/c range. For  $p_T > 9$  GeV/c, ASW and WHDG results show a better agreement with the 20-30% ( $N_{\text{part}} = 167$ ) centrality bin due to a slow decrease of  $v_2$  with  $p_T$  in this bin (see Fig. 1(b)). However, this seems to be accidental, since the  $v_2$  values for the other centrality bins remain large, and are significantly above the WHDG calculations (the p-value for the agreement is  $< 10^{-4}$ ).

In all these models, the inclusive suppression  $R_{\text{AA}}$  and

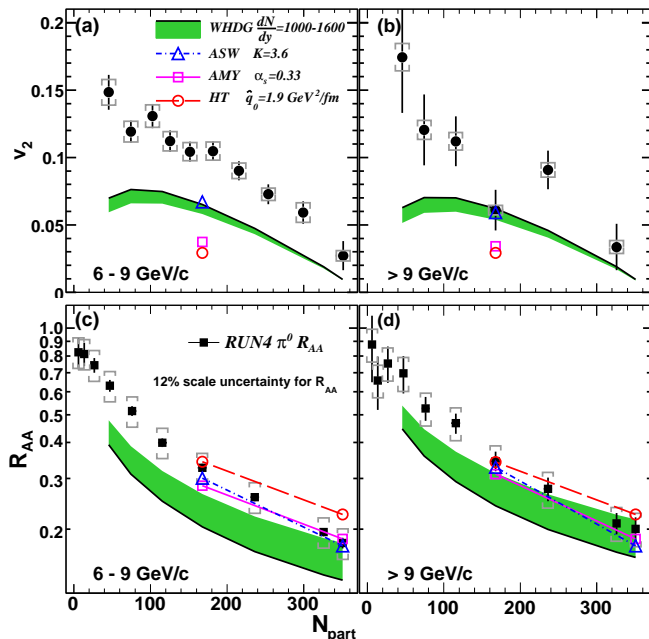


FIG. 2: (Color online) (a)-(b)  $v_2$  vs  $N_{\text{part}}$  in two  $p_T$  ranges; (c)-(d)  $R_{AA}$  vs  $N_{\text{part}}$  in same  $p_T$  ranges. Each are compared with four pQCD models from [8] (AMY, HT, ASW) and [22] (WHDG). Log-scale is used for  $R_{AA}$  to better visualize various model calculations. Note that the  $\frac{dN}{dg}=1000$  of WHDG corresponds to lower (upper) boundary of the shaded bands for  $v_2$  ( $R_{AA}$ ), while  $\frac{dN}{dg}=1600$  corresponds to upper (lower) boundary for  $v_2$  ( $R_{AA}$ ).

$v_2$  are anti-correlated, *i.e.* a smaller  $R_{AA}$  implies a larger  $v_2$  and vice versa. Consequently, more information can be obtained by comparing the data with a given model for both  $R_{AA}$  and  $v_2$ . Fig. 2 (c)-(d) compares the centrality dependence of  $\pi^0$   $R_{AA}$  data to four model calculations for the same two  $p_T$  ranges [21]. The calculations are available for a broad centrality range for WHDG, but only in 0-5% and 20-30% centrality bins for AMY, HT and ASW. The level of agreement varies among the models. The HT calculations are slightly above the data in the most central bin, while WHDG systematically underpredicts the data over the full centrality range, though better agreement with the data is obtained for  $p_T > 9$  GeV/c. On the other hand, ASW and AMY calculations agree with the data very well in both  $p_T$  ranges. The different levels of agreement among the models are partially due to their different trends of  $R_{AA}$  with  $p_T$ : WHDG and ASW results have stronger  $p_T$  dependences than what is implied by the data, and tend to deviate at low  $p_T$  when fitted to the full  $p_T$  range [7, 8]. Given the larger fractional systematic error for  $R_{AA}$  measurements compared to the  $v_2$  measurements, the deviation of  $v_2(N_{\text{part}})$  from the data is more dramatic than that for the  $R_{AA}(N_{\text{part}})$ . Nevertheless, Fig. 2 clearly shows the importance for any model to simultaneously describe the  $R_{AA}$  and the azimuthal anisotropy of the data.

The fact that the high  $p_T$   $v_2$  at RHIC exceeds expectation of pQCD jet-quenching models was first pointed out in Ref. [23] in 2002. This was not a serious issue back then since the  $p_T$  reach of early measurements was rather limited, and the  $v_2$  could be strongly influenced, up to 6 GeV/c for pions, by collective flow and recombination effects rather than jet quenching [27]. Fig. 2 clearly shows that the  $v_2$  at  $p_T$  above 6 or even 9 GeV/c still exceeds the pQCD-based energy loss models. It is possible that geometrical effects due to fluctuations and CGC effects, ignored in these models, can increase the calculated  $v_2$ ; it is also possible that the energy loss process in the sQGP has a steeper  $l$  dependence (*e.g.* AdS/CFT) than what is currently implemented in these models.

To test whether these two ideas could bridge the difference between data and theory, we compare the data with the JR model from [24]. This model is based on a naïve jet absorption picture with an exponential survival probability  $e^{-\kappa I}$  for jets, where the line integral  $I = \int dl \rho$  is chosen for a quadratic dependence of absorption in a longitudinally expanding medium, and  $\kappa$  is tuned to reproduce the central  $R_{AA}$  data. The medium density  $\rho$  is given by two leading candidates of the initial geometry: MC Glauber geometry  $\rho_{\text{GL}}(x, y) = 0.43\rho_{\text{part}}(x, y) + 0.14\rho_{\text{coll}}(x, y)$ , *i.e.* a mixture of participant density profile and binary collision profile from PHOBOS [25]; and MC CGC geometry  $\rho_{\text{CGC}}(x, y)$  of Drescher & Nara [14]. The effect of fluctuations for both profiles were included via the standard rotation procedure [13]. The short-dashed curves in Fig. 3(a) show that the result for Glauber geometry without rotation ( $\rho_{\text{GL}}$ ) compares reasonably well with those from WHDG [22] and a version of ASW model from [26]. Consequently, we use the JR model to estimate the shape distortions due to fluctuations and CGC effects. The results for Glauber geometry with rotation ( $\rho_{\text{GL}}^{\text{Rot}}$ ) and CGC geometry with rotation ( $\rho_{\text{CGC}}^{\text{Rot}}$ ) each lead to an  $\sim 15 - 20\%$  increase of  $v_2$  in mid-central collisions. However, these calculated results still fall below the data.

Figure 3(b) compares the same data with three JR models for the same matter profiles, but calculated for a line integral motivated by AdS/CFT correspondence  $I = \int dl l\rho$ . The stronger  $l$  dependence for  $\rho_{\text{GL}}$  significantly increases (by  $> 50\%$ ) the calculated  $v_2$ , and brings it close to the data for mid-central collisions. However, a sizable fractional difference in central bin seem to require additional increase from fluctuations and CGC geometry. Fig. 3 (b) also shows a CT model from [26], which implements the AdS/CFT  $l$  dependence within the ASW framework [29]; it compares reasonably well with the JR model for  $\rho_{\text{GL}}$  (short-dashed curves). Note that the CT or JR models in Fig. 3 have been tuned independently to reproduce the 0-5%  $\pi^0$   $R_{AA}$  data, and they all describe the centrality dependence of  $R_{AA}$  very well (see Fig. 3 (c)-(d)). On the other hand, these models predict a stronger suppression for dihadrons than for single hadrons, opposite to experimental findings [28], thus a

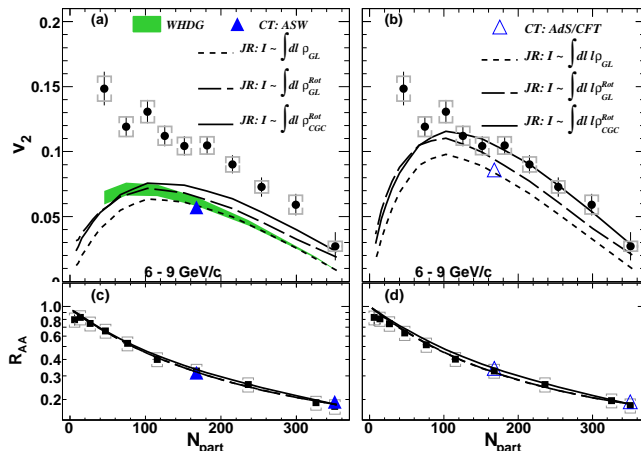


FIG. 3: (Color online)  $v_2$  vs  $N_{\text{part}}$  in 6-9 GeV/c compared with various models: (a) WHDG [22] (shaded bands), ASW [26] (solid triangle), and three JR calculations [24] with quadratic  $l$  dependence with longitudinal expansion for Glauber geometry (dashed lines), rotated Glauber geometry (long dashed lines) and rotated CGC geometry (solid lines); (b) Same as (a) except that AdS/CFT modified calculation in ASW framework (triangle) from [26] is shown and the JR calculations were done for cubic  $l$  dependence with longitudinal expansion; (c)-(d) the comparison of calculated  $R_{\text{AA}}$ s from these models with data.

global confrontation of any model with all experimental observables is warranted.

In summary, we presented results on  $\pi^0$  azimuthal anisotropy ( $v_2$ ) in  $1 < p_T < 18$  GeV/c in Au+Au collisions at  $\sqrt{s_{\text{NN}}}=200$  GeV. The measurements indicate sizable  $v_2(p_T)$  that decreases gradually for  $3 \lesssim p_T \lesssim 7 - 10$  GeV/c, but remains positive for  $p_T > 10$  GeV/c. This large  $v_2$  is striking in that it exceeds expectations of pQCD energy-loss models even at  $p_T \sim 10$  GeV/c. Estimates of the  $v_2$  increase due to modifications of initial geometry from gluon saturation effects and fluctuations indicate that they are insufficient to reconcile data and theory. Incorporating an AdS/CFT-like path-length dependence for jet quenching in a pQCD-based framework [26] and a schematic model [24] both compare well with the data. However, more detailed study beyond these simplified models are required to quantify the nature of the path-length dependence. Our precision data provide key experimental constraints on the role of initial geometry and for elucidating the jet quenching mechanism.

We thank the staff of the Collider-Accelerator and Physics Departments at BNL for their vital contributions. We acknowledge support from the Office of Nuclear Physics in DOE Office of Science and NSF (USA),

MEXT and JSPS (Japan), CNPq and FAPESP (Brazil), NSFC (China), MSMT (Czech Republic), IN2P3/CNRS and CEA (France), BMBF, DAAD, and AvH (Germany), OTKA (Hungary), DAE and DST (India), ISF (Israel), NRF (Korea), MES, RAS, and FAE (Russia), VR and KAW (Sweden), U.S. CRDF for the FSU, US-Hungary Fulbright, and US-Israel BSF.

\* Deceased

† PHENIX Spokesperson: jacak@skipper.physics.sunysb.edu

- [1] K. Adcox *et al.*, Nucl. Phys. A **757** (2005) 184; J. Adams *et al.*, Nucl. Phys. A **757** (2005) 102; B. B. Back *et al.*, Nucl. Phys. A **757** (2005) 28; I. Arsene *et al.*, Nucl. Phys. A **757** (2005) 1.
- [2] M. Gyulassy, I. Vitev, X. N. Wang and B. W. Zhang, arXiv:nucl-th/0302077.
- [3] K. Adcox *et al.*, Phys. Rev. Lett. **88**, 022301 (2002)
- [4] C. Adler *et al.* Phys. Rev. Lett. **90**, 082302 (2003)
- [5] A. Adare *et al.*, Phys. Rev. C **80**, 024908 (2009)
- [6] A. Majumder and M. Van Leeuwen, arXiv:1002.2206
- [7] A. Adare *et al.*, Phys. Rev. C **77**, 064907 (2008)
- [8] S. A. Bass *et al.* Phys. Rev. C **79**, 024901 (2009)
- [9] B. Muller, Prog. Theor. Phys. Suppl. **174**, 103 (2008).
- [10] S. Peigne and A. V. Smilga, Phys. Usp. **52**, 659 (2009)
- [11] S. S. Gubser, D. R. Gulotta, S. S. Pufu and F. D. Rocha, JHEP **0810**, 052 (2008);
- [12] M. L. Miller, K. Reygers, S. J. Sanders and P. Steinberg, Ann. Rev. Nucl. Part. Sci. **57**, 205 (2007)
- [13] B. Alver *et al.*, Phys. Rev. C **77**, 014906 (2008)
- [14] H. J. Drescher and Y. Nara, Phys. Rev. C **75**, 034905 (2007)
- [15] M. Luzum and P. Romatschke, Phys. Rev. C **78**, 034915 (2008) [Erratum-ibid. **79**, 039903 (2009)]
- [16] T. Hirano and Y. Nara, Phys. Rev. C **79**, 064904 (2009)
- [17] S. S. Adler *et al.*, Phys. Rev. Lett. **96**, 032302 (2006)
- [18] S. S. Adler *et al.*, Phys. Rev. C **76**, 034904 (2007)
- [19] S. Afanasiev *et al.*, Phys. Rev. C **80**, 054907 (2009)
- [20] A. Adare *et al.*, Phys. Rev. C **78**, 014901 (2008)
- [21] A. Adare *et al.*, Phys. Rev. Lett. **101**, 232301 (2008)
- [22] S. Wicks, W. Horowitz, M. Djordjevic and M. Gyulassy, Nucl. Phys. A **784**, 426 (2007);
- [23] E. V. Shuryak, Phys. Rev. C **66**, 027902 (2002)
- [24] A. Drees, H. Feng and J. Jia, Phys. Rev. C **71**, 034909 (2005); J. Jia and R. Wei, arXiv:1005.0645
- [25] B. B. Back *et al.* Phys. Rev. C **65**, 061901 (2002)
- [26] C. Marquet and T. Renk, Phys. Lett. B **685**, 270 (2010)
- [27] V. Greco, C. M. Ko and P. Levai, Phys. Rev. C **68**, 034904 (2003); R. J. Fries, B. Muller, C. Nonaka and S. A. Bass, Phys. Rev. C **68**, 044902 (2003)
- [28] A. Adare *et al.*, arXiv:1002.1077 [nucl-ex].
- [29] The two CT models (ASW and AdS/CFT) in Fig. 3 are based on a 3D ideal hydrodynamic code slightly different from that of the ASW model shown in Fig. 2.